International Journal Fracture manuscript No.
(will be inserted by the editor)

A fast algorithm for the elastic fields due to interacting fibre breaks in a periodic fibre composite

Ankit Gupta, Sivasambu Mahesh, Shyam M. Keralavarma

Received: date / Accepted: date

Abstract Monte Carlo simulations of the failure of unidirectional fibre composites typically require numerous evaluations of the stress-state in partially damaged composite patches. In a simulated composite patch comprised of N fibres, of which N_b fibres are broken in a common cross-sectional plane transverse to the fibre direction, the stress overloads in the intact fibres are given by the weighted superposition of the unit break solutions associated with each of the breaks. Determining the weights involves solving N_b linear equations, and determining overloads in the intact fibres requires matrix-vector multiplication. These operations require $O(N_b^3)$, and $O(NN_b)$ floating point operations, respectively. These costs become prohibitive for large N, and N_b; they limit Monte Carlo failure simulations to composite patches of only a few thousand fibres.

In the present work, a fast algorithm to determine the overloads in a partially damaged composite, requiring $O(N_b^{1/3} N \log N)$ floating point operations, is proposed. This algorithm is based on the discrete Fourier transform. The efficiency of the proposed method derives from the computational simplicity of weighted superposition in Fourier space. Computations of the stress state ahead of large circular clusters of breaks in composite patches comprised of about one million fibres are used to demonstrate the efficiency of the proposed algorithm.

Keywords Composites; Fracture; Algorithm; Discrete Fourier Transform; Numerical methods

Ankit Gupta · Sivasambu Mahesh (✉) · S. M. Keralavarma
Department of Aerospace Engineering, Indian Institute of Technology Madras, Chennai 600 036, India.
E-mail: smahesh@iitm.ac.in

1 Introduction

Monte-Carlo simulations are well-established as important tools in gaining insight into the strength distributions of idealised unidirectional polymer matrix composite materials Smith (1980); Beyerlein et al (1996); Zhou and Curtin (1995); Curtin (1998); Landis et al (2000); Mahesh et al (1999, 2002); Mahesh and Phoenix (2004); Habeeb and Mahesh (2015). In these simulations, sequential breakage of fibres, and load redistribution amongst surviving fibres is simulated up to the point of composite failure. Often, load redistribution is governed by the shear-lag model proposed for two- and three-dimensional fibre-reinforced composites by Hedgepeth (1961) and Hedgepeth and Van Dyke (1967), respectively. The Hedgepeth shear-lag model assumes that fibres transmit axial loads, while the matrix transmits shear stresses. The quantum of the shear-stress transmitted by a matrix element is proportional to the relative axial displacements of the fibres abutting it. The Hedgepeth shear-lag model yields the stress overloads due to a single break in a composite comprised of infinitely many fibres. Since Monte Carlo simulations, must necessarily be performed only on a finite composite 'patch', Landis et al (2000) proposed imposing periodic boundary conditions. The stress overloads due to a single break, as predicted by Landis et al (2000), are spatially periodic. A fast algorithm for their determination was recently given by Gupta et al (2017a).

When multiple breaks are present in a section transverse to the fibre direction, they must interact in order to ensure zero tractions at the breaks (Hedgepeth 1961; Hedgepeth and Van Dyke 1967; Beyerlein et al 1996; Mahesh et al 1999; Landis et al 2000; Mahesh et al 2002). Given the geometric and material linearity inherent in the Hedgepeth shear-lag model, the inter-

action amongst breaks will be linear. Each fibre break is thus assigned a weight, whose magnitude depends on all other breaks. Physically, the weight of a fibre break is proportional to its opening displacement (Beyerlein et al 1996).

Stress overloads on surviving fibres are given by the weighted superposition of the single break solutions. The determination of the weights of N_b breaks in the composite patch entails solving a dense system of N_b linear equations at a computational cost of $O(N_b^3)$. Performing the weighted superposition of the unit break solutions to obtain overloads on the intact fibres entails a further cost of NN_b. These computations also entail computer memory, which scales as $O(N_b^2)$. These costs become prohibitive when $N_b \to N$ and N becomes large, and limit the composite sizes treated in Monte Carlo simulations to a few thousand fibres.

Another approach, viz., tree codes (Pfalzner and Gibbon 2005), developed in the astrophysical literature to treat the interactions between N bodies distributed arbitrarily in space has been applied in the present context of fibre composites by the present authors (Gupta et al 2017b). In this method, interactions between nearby breaks are treated exactly. Clusters of distant breaks, on the other other hand, are lumped together into a single super-break. Interactions between super-breaks are then accounted for. This device reduces the total number of interactions that must be treated, and enables Monte Carlo simulations of larger patches than previously possible. Gupta et al (2017b) performed Monte-Carlo simulations on patches with up to $N = 2^{16} = 65536$ fibres. Treecode based Monte Carlo simulation involves a small, but non-zero error that arises from lumping together distant breaks.

In the present work, an exact and fast algorithm to compute the overloads due to an arbitrary number of breaks in large patches is proposed. The fast algorithm is based on performing the weighted superposition of influences of individual breaks in Fourier space, wherein this computation is much more efficient. Transformation from real to Fourier space and back are effected using the discrete Fourier transform, costing $O(N \log N)$ floating point operations. Weights are determined iteratively using the conjugate gradient algorithm (Greenbaum 1997). Each iteration of this algorithm again involves weighted superposition of influences, using progressively better approximations of the weights. The number of iterations is empirically found to scale as $O(N_b^{1/3})$. The total computational cost thus scales as $O(N_b^{1/3})\ O(N \log N)$, and the memory requirement scales as $O(N)$. For all but small N_b, no more than a few hundred breaks, the exact computations based on the present method are shown to be faster than those using the direct method. The present method is also faster than the treecode based method for all N_b.

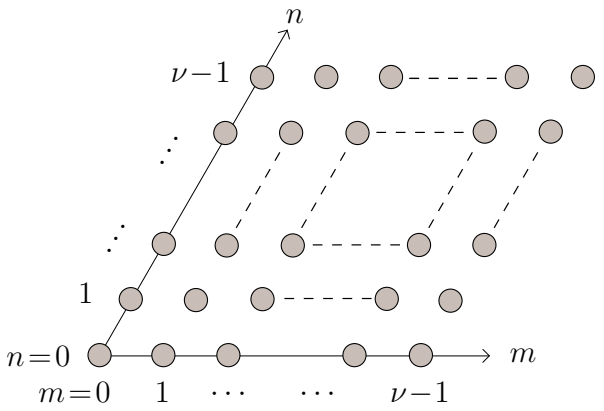

Fig. 1: A rhombus-shaped periodic patch of $\nu \times \nu$ fibers arranged in a hexagonal lattice showing the m–n coordinate system (Sec. 2.1).

2 Model and algorithm

2.1 The influence matrix and its diagonal form

As in Gupta et al (2017a), a rhombus-shaped finite 'patch' comprised of $N = \nu^2$ fibers arranged in a hexagonal lattice, as depicted in Fig. 1 (a), is taken to represent the cross-section of the unidirectional composite. Two edges of the rhombus define the m, and n coordinate axes. Following Landis et al (2000), the following periodicity conditions are imposed: fibers $(0, n)$ and $(\nu - 1, n)$ (the left and right edges of the patch) are assumed adjacent for all $n \in \{0, 1, \ldots, \nu - 1\}$. Similarly, fibers at the top $(n = \nu - 1)$ and bottom $(n = 0)$ edges are also considered adjacent. On account of periodicity, only fibre indices modulo ν are significant. For any integer a, these are defined as

$$[a] := a - \nu \lfloor a/\nu \rfloor . \tag{1}$$

Here, $\lfloor a/\nu \rfloor$ denotes the largest integer no greater than a/ν.

Let K_{mn} denote the stress concentration in fibre (m, n) in a transverse plane, due to a single break in fibre $(0, 0)$ located in the same transverse plane. The stress concentration is the load in fibre (m, n) normalised by the far-field load, and can therefore be no smaller than unity. The stress overload, Ω_{mn} is defined as $\Omega_{mn} = K_{mn} - 1$. It is clear that $\Omega_{mn} \geq 0$. A fast algorithm to determine Ω_{mn} for large patch sizes ν has been given by Gupta et al (2017a).

Let $[\Lambda]$ denote an influence matrix of the composite patch, and let Λ_{mnpq} be the overload at fibre (m, n) at

a cross-section due to a single break in fibre (p, q), at the same cross-section. Because of the assumed periodicity of the patch, stress overloads obey the following important translation invariance property: The stress overload on fibre (m, n) due to a single break located at fibre (p, q) is given by $\Omega_{[m-p],[n-q]}$ (Landis et al 2000; Mahesh et al 2002; Gupta et al 2017a). Therefore,

$$\Lambda_{mnpq} = \Omega_{[m-p],[n-q]}. \tag{2}$$

The fourth order matrix Λ_{mnpq} is circulant along two disjoint pairs of modes, following the terminology of Rezghi and Eldén (2011). Consider the second order matrix Λ_{MnPq}, obtained by fixing $m = M$, and $p = P$, for some $0 \leq M, P \leq \nu - 1$. Then, following the definition of Rezghi and Eldén (2011, Def. (4.2)), Eq. (2) implies that Λ_{MnPq} is circulant in the pair of modes $\{2, 4\}$, as it satisfies the property:

$$\Lambda_{MnPq} = \Lambda_{Mn'Pq'}, \quad \text{if } [n - q] = [n' - q'] \tag{3}$$

Similarly, it can be shown that Λ_{mNpQ} obtained by fixing $n = N$ and $q = Q$ for some $0 \leq N, Q \leq \nu - 1$, is also circulant in the pair of modes $\{1, 3\}$.

Circulant matrices, Λ_{MnPq} and Λ_{mNpQ}, can be diagonalized by the unitary Fourier matrix (Davis 2012), F_ν. In terms of $\omega_\nu = \exp(2\pi i/\nu)$, where $i = \sqrt{-1}$, the Fourier matrix is defined as:

$$F_\nu = \frac{1}{\sqrt{\nu}} \begin{pmatrix} 1 & 1 & 1 & \dots\dots & 1 \\ 1 & \omega_\nu & \omega_\nu^2 & \dots\dots & \omega_\nu^{\nu-1} \\ 1 & \omega_\nu^2 & \omega_\nu^4 & \dots\dots & \omega_\nu^{2(\nu-1)} \\ \dots & \dots & \dots & \dots\dots & \dots \\ \dots & \dots & \dots & \dots\dots & \dots \\ 1 & \omega_\nu^{\nu-1} & \omega_\nu^{2(\nu-1)} & \dots\dots & \omega_\nu^{(\nu-1)^2} \end{pmatrix}. \tag{4}$$

Numbering the rows and columns in the range $m, n \in \{0, 1, \dots, \nu - 1\}$, it is clear from Eq. (4) that $F_{\nu;mn} = \omega_\nu^{mn}/\sqrt{\nu}$. For clarity, the subscript ν in F_ν and ω_ν are suppressed henceforth. Also, unless otherwise specified, summation over repeated Latin indices over the range $\{0, 1, 2, \dots, \nu - 1\}$ is implied henceforth.

Rezghi and Eldén (2011, Theorem 5.2) have shown that the higher order matrix Λ_{mnpq} can also be diagonalised in the disjoint modes $\{1, 3\}$ and $\{2, 4\}$. Thus, if $\overline{F}_{ij}$ denotes the complex conjugate of F_{ij},

$$\begin{aligned} \hat{\Lambda}_{abcd} &= \overline{F}_{am}\, \overline{F}_{bn}\ \Lambda_{mnpq}\ F_{pc}\, F_{qd} \\ &= \frac{1}{\nu^2}\, \omega^{-am}\, \omega^{-bn}\ \Lambda_{mnpq}\ \omega^{pc}\, \omega^{qd}, \end{aligned} \tag{5}$$

represents a diagonal matrix in the modes $\{1, 3\}$ and $\{2, 4\}$. This means that $\hat{\Lambda}_{abcd} = 0$, if $a \neq c$, or $b \neq d$. However, if $a = c$, and $b = d$, $\hat{\Lambda}_{abab} \neq 0$ (no sum), in general. Setting $\hat{D}_{ab} = \hat{\Lambda}_{abab}$ (no sum), Rezghi and Eldén (2011, Theorem 5.2) show that

$$\begin{aligned} \hat{D}_{ab} &= \nu \bar{F}_{am} \bar{F}_{bn} \Lambda_{mn00}, \\ &= \omega^{-am}\, \omega^{-bn}\ \Omega_{mn}. \end{aligned} \tag{6}$$

The two dimensional discrete Fourier transform of Ω_{mn} is defined following Briggs and Henson (1995, p. 146) as

$$\hat{\Omega}_{ab} = \frac{1}{\nu^2} \omega^{-am}\, \omega^{-bn}\ \Omega_{mn}. \tag{7}$$

Comparing Eqs. (6) and (7) reveals that

$$\hat{D}_{ab} = \nu^2 \hat{\Omega}_{ab}. \tag{8}$$

2.2 Weighted superposition of overloads

Let an arbitrary set $\mathcal{B}$ of fibres be broken in a common plane transverse to the fibre direction. Let the weights, w_{pq}, corresponding to these breaks be known. Then, the overload at any other fibre, (m, n), whether broken or intact, is given by a weighted superposition of the single break solutions corresponding to each of the breaks:

$$\Phi_{mn} = \sum_{(p,q)\in\mathcal{B}} \Lambda_{mnpq} w_{pq}. \tag{9}$$

Since the weights of broken and intact fibres satisfy (Beyerlein et al 1996),

$$w_{pq} \begin{cases} = 0, & \text{if } (p, q) \notin \mathcal{B}, \\ > 0, & \text{if } (p, q) \in \mathcal{B}, \end{cases} \tag{10}$$

Eq. (9) can be written as

$$\Phi_{mn} = \Lambda_{mnpq} w_{pq}. \tag{11}$$

Here, summation is implied over all $p, q \in \{0, 1, \dots, \nu - 1\}$. The direct evaluation of overloads, Φ_{mn} using Eq. (11) involves $O(\nu^4)$ floating point operations.

It is now shown that the number of floating point operations can be drastically reduced by performing the matrix-vector multiplication of Eq. (11) in Fourier space. To this end, consider the two-dimensional Fourier transform (Eq. (7)) of w_{pq}:

$$\hat{w}_{cd} = \frac{1}{\nu^2} \omega^{-rc} \omega^{-sd} w_{rs}. \tag{12}$$

Observing that

$$\frac{\omega^{pc}}{\sqrt{\nu}} \frac{\omega^{-rc}}{\sqrt{\nu}} = F_{pc} \bar{F}_{cr} = \delta_{pr} = \begin{cases} 1, & \text{if } p = r, \\ 0, & \text{if } p \neq r. \end{cases}$$

because F is unitary, it follows from Eqs. (5) and (12) that

$$\begin{aligned}\hat{\Lambda}_{abcd}\hat{w}_{cd} =& \frac{1}{\nu^2}\omega^{-am}\omega^{-bn}\Lambda_{mnpq}w_{pq},\\ =& \frac{1}{\nu^2}\omega^{-am}\omega^{-bn}\Phi_{mn}.\end{aligned} \tag{13}$$

Eq. (11) has been employed in obtaining the second equality in Eq. (13). Expressed in words, Eq. (13) states that $\hat{\Lambda}_{abcd}\hat{w}_{cd}$ is the Fourier transform of Φ_{mn}. Φ_{mn} is then obtained using the inverse Fourier transform (Briggs and Henson 1995, p. 146) as

$$\Phi_{mn} = \omega^{ma}\omega^{nb}\left(\hat{\Lambda}_{abcd}\hat{w}_{cd}\right). \tag{14}$$

On account of properties established in Eqs. (6), and (8), the ab-th element of the term within brackets in Eq. (14),

$$\left(\hat{\Lambda}_{abcd}\hat{w}_{cd}\right) = \nu^2\hat{\Omega}_{ab}\hat{w}_{ab}, \tag{15}$$

with no summation in the right side over indices a and b. The right side thus represents an element-wise product of two $\nu\times\nu$ matrices, $\hat{\Omega}_{ab}$, and $\hat{w}_{ab}$.

The computation of $\nu^2\hat{\Omega}_{ab}\hat{w}_{ab}$ (no sum) requires $O(\nu^2)$ floating point operations. The inverse Fourier transform of Eq. (14) is known to require $O(\nu^2\log\nu^2)$ operations (Briggs and Henson 1995). This is also the asymptotic computational cost of the direct Fourier transforms of Ω_{mn} and w_{pq} in Eqs. (7) and (12), respectively. The computation of Φ_{mn} by Fourier transformation is thus more efficient computationally ($O(\nu^2\log\nu^2) = O(N\log N)$ floating point operations) than by direct multiplication ($O(\nu^4) = O(N^2)$ operations). $\hat{\Omega}_{ab}$, and $\hat{w}_{ab}$ appearing in Eq. (15) must be stored in memory. The memory requirement thus scales as $O(N)$.

2.3 Determination of weights

In Sec. 2.2, a method for fast weighted superposition of single break solutions was developed. This method is now used to speed up the determination of weights of an arbitrary set of broken fibres.

The weights of broken fibres w_{pq}, for $(p,q)\in\mathcal{B}$ are determined by requiring that the fibre breaks be traction free (Hedgepeth 1961; Hedgepeth and Van Dyke 1967; Beyerlein et al 1996; Mahesh et al 1999; Landis et al 2000), i.e.,

$$\Phi_{mn} = \sum_{(p,q)\in\mathcal{B}}\Lambda_{mnpq}w_{pq} = -1, \text{ for all } (m,n)\in\mathcal{B}. \tag{16}$$

In order to use available techniques for solving matrix equations, Λ_{mnpq} is first converted into a second order matrix using the following contractions: $\alpha = n+m\nu$, and $\beta = q+p\nu$; $\alpha,\beta\in\mathscr{A} = \{0,1,2,\ldots,\nu^2-1\}$. Indices α and β now refer to specific fibres; $\mathscr{A}$ refers to the set of all fibres. In the following, repeated Greek indices indicate summation over the range $\mathscr{A}$, e.g., when expressed in terms of the contracted indices, Eq. (11) becomes

$$\Phi_\alpha = \Lambda_{\alpha\beta}w_\beta. \tag{17}$$

The set of all broken fibres, expressed in terms of the contracted indices is

$$\mathscr{B} = \{\beta = q+p\nu : (p,q)\in\mathcal{B}\}. \tag{18}$$

In terms of $\mathscr{B}$, Eq. (16) becomes

$$\Phi_\alpha = \sum_{\beta\in\mathscr{B}}\Lambda_{\alpha\beta}w_\beta = -1, \text{ for all } \alpha\in\mathscr{B}. \tag{19}$$

The matrix of elements $\Lambda_{\alpha\beta}$ possesses the desirable properties of symmetry and negative definiteness (Gupta et al 2017a). Eq. (19), rewritten as

$$\sum_{\beta\in\mathscr{B}}(-\Lambda_{\alpha\beta})w_\beta = +1, \text{ for all } \alpha\in\mathscr{B}, \tag{20}$$

is therefore amenable to iterative solution using the conjugate gradients algorithm (Greenbaum 1997). Starting with an initial guess at iteration $\iota = 0$, say $w_\beta^{(0)} = 1$, for all $\beta\in\mathscr{B}$, the conjugate gradient algorithm generates successive improved approximations to the solution vector, $\{w_\beta^{(\iota)}\}$ in each iteration ι. Iterations are terminated when a convergence condition is satisfied.

Much of the computational effort in a typical conjugate gradient iteration, ι, is concentrated into computing the matrix-vector product, $\sum_{\beta\in\mathscr{B}}\Lambda_{\alpha\beta}w_\beta^{(\iota)}$, for all $\alpha\in\mathscr{B}$. It follows from Eqs. (10) and (19) that $w_\beta = 0$, if $\beta\notin\mathscr{B}$. Thus, the computationally intensive matrix-vector product can also be written as $\Lambda_{\alpha\beta}w_\beta^{(\iota)}$, for all $\alpha\in\mathscr{B}$. But this is precisely the restriction to $\alpha\in\mathscr{B}$, of the product in Eq. (17) with $w_\beta = w_\beta^{(\iota)}$. A method for its fast $O(N\log N)$ computation has already been developed in Sec. 2.2. In other words, each conjugate gradient iteration, and therefore, the conjugate gradient method itself stands to be drastically speeded up by exploiting the discrete Fourier transform based overload calculation developed in Sec. 2.2.

3 Results

The fast algorithm developed in Sec. 2 to compute the stress overloads in a unidirectional composite cross-section

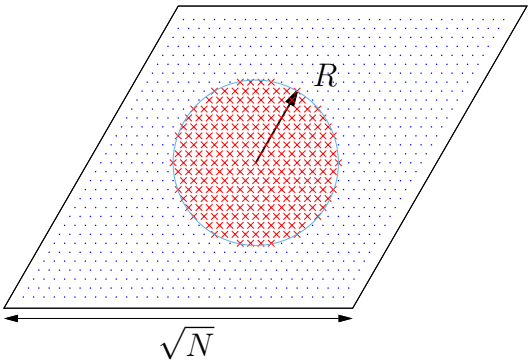

Fig. 2: A circular cluster of breaks of radius R (red crosses) in a patch of N fibres. Intact fibres are indicated by blue dots. All distances are normalised by the centre-to-centre spacing of adjacent fibres in the hexagonal lattice.

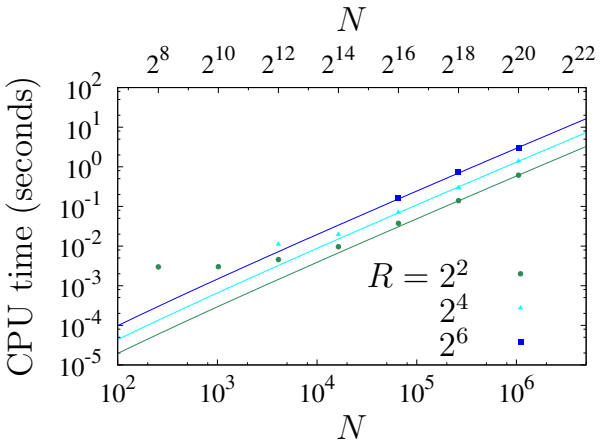

Fig. 3: Scaling of CPU time, t, required to calculate weights, with composite patch size. Timing data for patches of sizes $N = \{2^8, 2^{10}, 2^{12}, 2^{14}, 2^{16}, 2^{18}, 2^{20}\}$ are shown. Broken fibres are arranged as circular clusters of radius R, for $R \in \{2^2, 2^4, 2^6\}$, which correspond to $N_b \in \{61, 931, 14845\}$ fibers breaks, respectively. The solid lines obey $t \propto N \log N$.

containing an arbitrary set of fibre breaks has been implemented in the `Octave` programming language (Eaton et al 2015), which calls the `FFTW3` library (Frigo and Johnson 2005) to perform fast Fourier transforms. A method implementing direct solution for the weights, using Cholesky factorisation of the interaction matrix through calls to the `LAPACK` library (Anderson et al 1999) has also been implemented in `Octave`. CPU times required by these implementations, when executed on the same workstation computer, are reported below.

Conjugate gradient iterations are terminated when the absolute norm of the residual vector drops below a tolerance of 10^{-6}. The number of iterations, I, required for the conjugate gradient algorithm to converge depends on the eigenvalues of the matrix (Greenbaum 1997). The matrix $\Lambda_{\alpha\beta}$, $\alpha, \beta \in \mathscr{A}$, has zero row sums (Beyerlein et al 1996), and is hence singular. For a fixed number of breaks, $N_b < N$, the row sums, and therefore, the smallest eigenvalue of the matrix $-\Lambda_{\alpha\beta}$, $\alpha, \beta \in \mathscr{B}$ (in Eq. (20)), most closely approaches zero, when the breaks are located nearest each other. A nearly circular cluster therefore represents the most computationally intensive arrangement of N_b breaks. This motivates considering circular clusters of broken fibres in the following, as shown schematically in Fig. 2. The unit of distance in the following is taken to the centre-to-centre spacing between adjacent fibres in the hexagonal lattice. The radius R of the circular cluster of breaks in Fig. 2 is specified as a multiple of this unit.

Fig. 3 shows the CPU time required to calculate the weights of all the broken fibres making up a circular cluster of radius R in a patch with N fibres. The green, cyan and blue solid lines obey $t = k(N \log N)$, where $k = 4.2\times10^{-8}$ s, 9.5×10^{-8} s, and 2.1×10^{-7} s, respectively. For small N, the CPU times do not scale as $O(N \log N)$. This is because, for small N, the computational time associated with fast Fourier transformation is smaller than or comparable to that of computational overheads, such as memory allocation, and initialisation of arrays. For $N \geq 2^{14}$, however, the computational time of fast Fourier transformation dominates. In this regime of large N, the scaling predicted by the asymptotic computational effort calculation of Sec. 2.2 is realised in the actual computation for fixed N_b.

For a patch of fixed size N, the smallest eigenvalue of the matrix of interest, $-\Lambda_{\alpha\beta}$, $\alpha, \beta \in \mathscr{B}$, approaches zero as the number of breaks, N_b, increases. The number of iterations of the conjugate gradient algorithm, I, and hence, computational time, must therefore increase with N_b (Greenbaum 1997). Fig. 4a shows the observed rate of increase, for three fixed N. The cyan, red and violet solid lines indicate curve fits of the scaling relationship, and correspond to $t \propto N_b^{0.28}$, $t \propto N_b^{0.31}$, and $t \propto N_b^{0.30}$, respectively. It is seen that for fixed N, CPU time t required to compute weights scales approximately as $t \sim N_b^{1/3}$. It is seen that the scaling exponent is not sensitive to N.

The number of conjugate gradient iterations, I corresponding to various N_b is shown in Fig. 4b for $N = 2^{20}$. The number of iterations also scales approximately as $I \propto N_b^{0.30}$, for large N_b. It follows that increases in the number of iterations, I, accounts entirely for increasing CPU time with increasing N_b. The time per iteration remains nearly fixed, regardless of N_b.

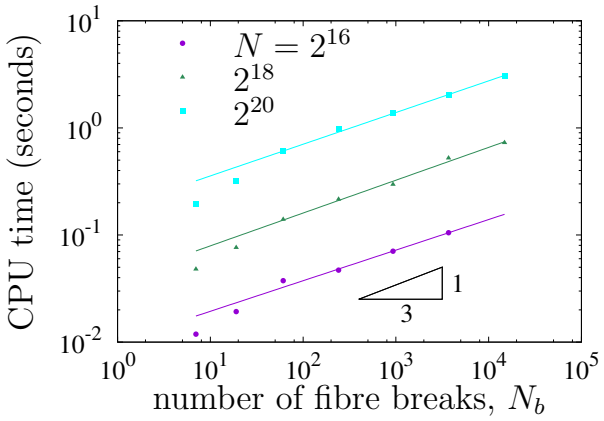

(a) Scaling of CPU time with N_b

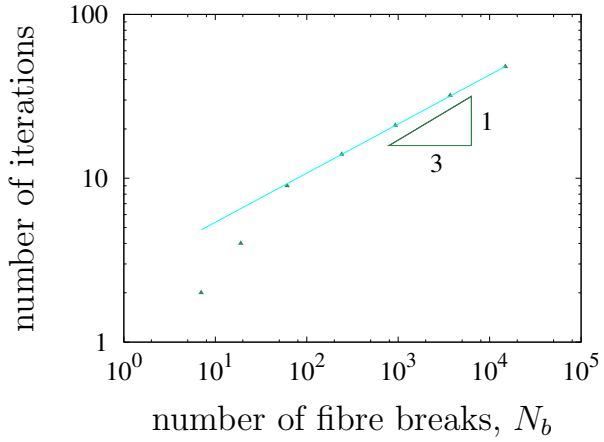

(b) Scaling of the number of conjugate iterations with N_b

Fig. 4: (**a**) Scaling of CPU time, t, required to calculate weights, with the number of breaks, N_b, for fixed patch sizes, $N \in \{2^{16}, 2^{18}, 2^{20}\}$. (**b**) Scaling of the number of conjugate gradient iterations, I, required to calculate weights, for $N = 2^{20}$. Breaks are arranged in the form of a circular cluster of radius $R \in \{2^1, 2^2, 2^3, 2^4, 2^5, 2^6,$ and $2^7\}$ ($N_b \in \{7, 19, 61, 241, 931, 3697, 14845\}$, respectively).

Computation time requirements for the methods to determine overloads due to a circular cluster of breaks are now directly compared. The three methods are the direct method, which involves Cholesky factorisation to determine the weights of broken fibres and $N \times N_b$ matrix-vector multiplication for the overloads (Beyerlein et al 1996), the tree code based method of Gupta et al (2017b), and the present DFT method. The parameter, θ, which is used to discriminate near and far interactions is taken to be 0.5. CPU times required to compute overloads in a patch of $N = 2^{14}$ fibres are shown in Fig. 5. Fig. 5a shows that the direct method is faster for $N_b < 585$. But CPU time corresponding to the direct method scales as $N_b^{2.7} \approx N_b^3$; the corre-

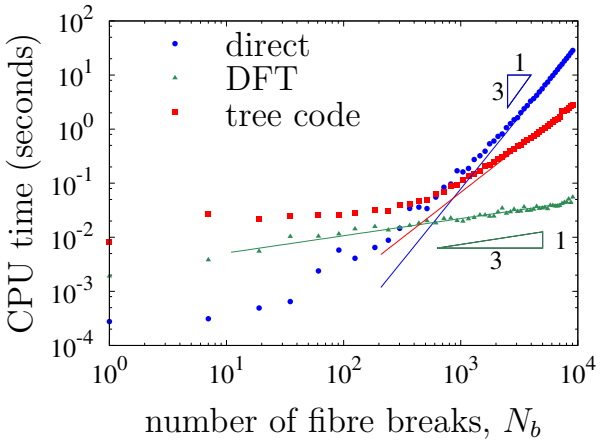

(a) Total time

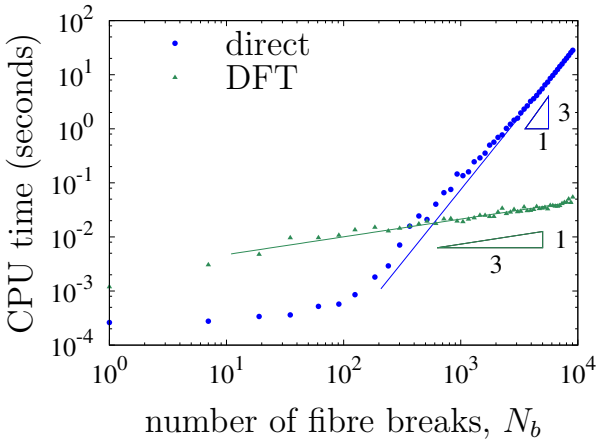

(b) Time for weights computation (Sec. 2.3)

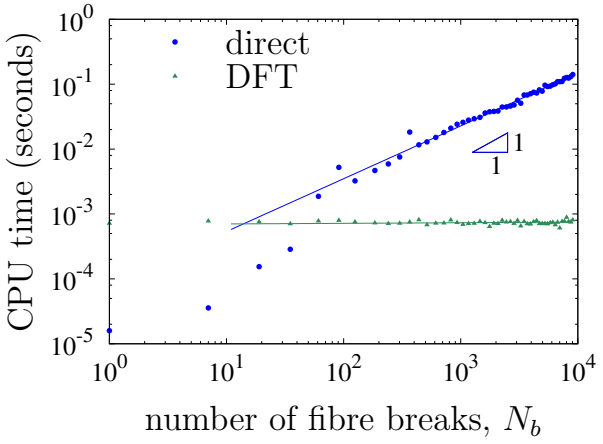

(c) Time for overloads computation (Sec. 2.2)

Fig. 5: Scaling of CPU time, t, with the number of broken fibres, N_b for (**a**) both weights and overloads, (**b**) weights, and (**c**) overloads computation. Times required for direct solution, tree code based solution, and using the present fast algorithm are compared. In all cases, the simulation patch is of size, $N = 2^{14}$.

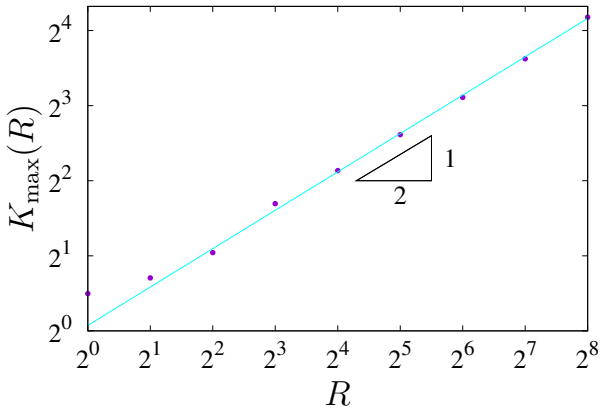

Fig. 6: The scaling of the maximum stress concentration with different cluster radii, $R = 2^0, 2^1, \ldots, 2^8$. The composite patch is comprised of $N = 2^{20}$ fibres. The cyan solid line obeys Eq. (22).

sponding scaling for the DFT method is found to be $N_b^{0.32} \approx N_b^{1/3}$. For $N_b \geq 585$ the DFT method is faster. At $N_b = 10^4$, the DFT method is nearly three orders of magnitude faster than the direct method. These observations clearly indicate the superiority of the DFT method for large N, and N_b.

Fig. 5a also shows that the total time for overload computation required by the present DFT method is smaller than that required by the treecode method (Gupta et al 2017b). For large N_b, the treecode time scales as $N_b^{1.68} \approx N_b^{5/3}$ The present DFT method is thus asymptotically faster than the treecode method. It is also more accurate, as it does not lump interactions between distant break.

Fig. 5b shows the CPU times required to determine the weights of breaks. The $O(N_b^3)$, and $O(N_b^{1/3})$ scalings expected for weights computation by the direct and DFT methods, respectively, are realised approximately. The actual scalings follow $O(N_b^{2.7})$ and $O(N_b^{0.33})$, respectively. Fig. 5c shows the CPU times required to compute overloads on intact fibres. The CPU times for the direct method scale in accord with the expected $O(NN_b)$. Also, the CPU times for the DFT method remain nearly constant with N_b. This is consistent with the expected independence of CPU time on N_b. It is also noticed that the CPU times for overload computation are orders of magnitude smaller than those for determining weights.

Consider a patch with a circular cluster of breaks of radius R, denoted $\mathcal{B}_R$. The maximum stress concentration in this patch,

$$K_{\max}(R) = \max_{(m,n)\notin\mathcal{B}_R} K_{mn}. \tag{21}$$

Fig. 6 plots the variation of $K_{\max}(R)$, for $R = 2^0$, 2^1, $\ldots$, 2^8, in a patch of $N = 2^{20}$ fibres. It is seen that

$$K_{\max} = 0.59\sqrt{\pi R} \approx \sqrt{\pi R/3}. \tag{22}$$

This agrees with the scaling of stress-intensity with the radius of a penny shaped crack in linear elastic fracture mechanics (Kanninen and Popelar 1985). A similar scaling was suggested by Mahesh et al (1999), but on the basis of calculations extending only up to $R = 20$.

4 Discussion

A fast algorithm has been proposed to determine the overloads on intact fibres due to broken fibres contained in the transverse section of a unidirectional composite loaded in the tension along the fibre direction. The equations governing the present model of the composite are very different from Kirchhoff's equations governing the voltages in a disordered resistor-fuse network (Alava et al 2006). Nevertheless, the present algorithm resembles the Fourier accelerated iterative solution algorithm proposed by Batrouni et al (1986), and Batrouni and Hansen (1988) for solving the electrical problem.

The Fourier accelerated technique (Batrouni et al 1986; Batrouni and Hansen 1988) involves introducing a circulant matrix, $[\epsilon]$, where $\epsilon_{\alpha\beta}$ scales as a power of the distance between nodes α and β. The power is selected so as to yield the greatest computational acceleration. The product of the circulant $[\epsilon]$ and the vector of Kirchhoff residuals at all the nodes, in Fourier space can then be computed very efficiently. This accelerates convergence of the iterative scheme. Other approaches proposed in the literature, aimed at pre-conditioning the coefficient matrix using Toeplitz (O'Shaughnessy and Procaccia 1985), optimal circulant (Chan and Ng 1996) and block circulant matrices (Nukala and Simunovic 2004), also employ a conceptually similar devise.

While the present algorithm is Fourier accelerated, in the sense of Batrouni et al (1986), and Batrouni and Hansen (1988), there are significant differences. First, their $\epsilon_{\alpha\beta}$ is a tuneable computational devise. Its analog in the present work, $\Lambda_{\alpha\beta}$, is determined by the structure of the present problem, and cannot be tuned. Second, Batrouni and Hansen (1988) perform their conjugate gradient iterations in Fourier space, so that successive iterates of the unaccelerated and accelerated algorithms are different. Presently, the conjugate gradient algorithm itself is implemented in its standard form (Greenbaum 1997); only the generation of conjugate gradient iterates has been made more efficient by performing it in Fourier space.

In later work, Batrouni et al (2002) used the Fourier accelerated method to solve the mechanical problem of

failure of a glued joint between infinitely long rigid and elastic substrates. The present model and Fourier accelerated algorithm closely resemble those associated with the lattice model of the glued joint. As in Batrouni et al (2002), the conjugate gradient method is used presently for solving the simultaneous equations in real space. Batrouni et al (2002) exploited the diagonal character of the infinite Green's function in Fourier space to accelerate the computation of the matrix vector multiplication within each conjugate gradient iteration. This devise is also employed in the present work. However, the use of the infinite Green's function in Batrouni et al (2002) to determine the redistribution of load over a finite patch entails a truncation error that decreases with patch size, and increases with the number of broken elements. This is because, in their setting, a part of the load dropped by elements in the simulation patch will redistribute amongst fictitious elements outside the patch. This load leakage from the patch increases with the number of broken elements, and their proximity to the edges of the finite patch. In the present work, this limitation is overcome by adopting periodic boundary conditions, and by developing a diagonalisation of the resulting circulant influence coefficient matrix in Fourier space. The present scheme is thus not affected by truncation error, and load leakage.

Algorithms based on direct solution of the governing equations in the case of the disordered resistor-fuse network have been proposed (Alava et al 2006; Nukala et al 2005). These algorithms are found to be even faster than the Fourier accelerated iterative algorithms. However, these algorithms exploit the sparsity of the Kirchhoff coefficient matrix. The present coefficient matrix, $\Lambda_{\alpha\beta}$, is not sparse, and is therefore, not amenable to such treatment.

5 Conclusion

Monte Carlo simulations of fibre composites have been extensively used in the literature to yield insights into the failure modes and strength scalings with patch size. The simulations are useful indicators of the failure modes when the size of the critical failure event is substantially smaller than that of the patch. If the size scale of the critical event becomes comparable to, or exceeds the patch size, edge effects dominate the observed failure mode. It is therefore, useful to be able to efficiently simulate the failure of large composite patches.

Computational limitations, however, have restricted simulation patches to a few thousand fibres in the literature. These limitations arise on account of the computational effort associated with determining (i) the stress overloads due to a single break in a large patch, (ii) the calculation of weights of a set of interacting breaks, and (iii) overloads on intact fibres by weighted superposition of the break influences. A solution for problem (i) by way of a fast algorithm was given by Gupta et al (2017a).

The present work proposes a discrete Fourier transform based method to substantially speed up (iii) above, for the case that fibre breaks are confined to a plane transverse to the fibre direction. Since the computationally time consuming aspect of problem (ii) above involves the repeated execution of (iii), (ii) is also speeded up. The calculation is computationally exact, and much faster than previous approaches for large patch sizes. Extensive studies of the computation time required to perform calculations (i) and (ii) above suggest that Monte Carlo simulations on composites comprised of as many as a million fibres should be feasible. However, the simulations themselves, and statistical interpretation of their results are left to future work.

References

Alava MJ, Nukala PK, Zapperi S (2006) Statistical models of fracture. Advances in Physics 55(3-4):349–476

Anderson E, Bai Z, Bischof C, Blackford S, Demmel J, Dongarra J, Du Croz J, Greenbaum A, Hammarling S, McKenney A, Sorensen D (1999) LAPACK Users' Guide, 3rd edn. SIAM, Philadelphia, PA

Batrouni GG, Hansen A (1988) Fourier acceleration of iterative processes in disordered systems. Journal of statistical physics 52(3-4):747–773

Batrouni GG, Hansen A, Nelkin M (1986) Fourier acceleration of relaxation processes in disordered systems. Physical review letters 57(11):1336

Batrouni GG, Hansen A, Schmittbuhl J (2002) Heterogeneous interfacial failure between two elastic blocks. Physical Review E 65(3):036,126

Beyerlein IJ, Phoenix SL, Sastry AM (1996) Comparison of shear-lag theory and continuum fracture mechanics for modeling fiber and matrix stresses in an elastic cracked composite lamina. International Journal of Solids and Structures 33(18):2543–2574

Briggs WL, Henson VE (1995) The DFT: An Owners' Manual for the Discrete Fourier Transform. SIAM

Chan RH, Ng MK (1996) Conjugate gradient methods for toeplitz systems. SIAM review 38(3):427–482

Curtin W (1998) Size scaling of strength in heterogeneous materials. Physical Review Letters 80(7):1445

Davis PJ (2012) Circulant matrices. American Mathematical Soc.

Eaton JW, Bateman D, Hauberg S, Wehbring R (2015) GNU Octave version 4.0.0 manual: a high-level interactive language for numerical computations. CreateSpace Independent Publishing Platform, URL http://www.gnu.org/software/octave/doc/interpreter

Frigo M, Johnson SG (2005) The design and implementation of fftw3. Proceedings of the IEEE 93(2):216–231

Greenbaum A (1997) Iterative methods for solving linear systems. SIAM

Gupta A, Mahesh S, Keralavarma SM (2017a) A fast algorithm for the elastic fields due to a single fiber break in a periodic fiber-reinforced composite. International Journal of Fracture 204(1):121–127

Gupta A, Mahesh S, Keralavarma SM (2017b) Strength distribution of large unidirectional composite patches with realistic load sharing. Physical Review E 96:043,002

Habeeb CI, Mahesh S (2015) Strength distribution of planar local load-sharing bundles. Physical Review E 92(2):022,125

Hedgepeth JM (1961) Stress concentrations in filamentary structures. NASA TN D-882

Hedgepeth JM, Van Dyke P (1967) Local stress concentrations in imperfect filamentary composite materials. Journal of composite materials 1(3):294–309

Kanninen MF, Popelar CL (1985) Advanced fracture mechanics. Oxford University Press

Landis CM, Beyerlein IJ, McMeeking RM (2000) Micromechanical simulation of the failure of fiber reinforced composites. Journal of the Mechanics and Physics of Solids 48(3):621–648

Mahesh S, Phoenix S (2004) Lifetime distributions for unidirectional fibrous composites under creep-rupture loading. International journal of fracture 127(4):303–360

Mahesh S, Beyerlein IJ, Phoenix SL (1999) Size and heterogeneity effects on the strength of fibrous composites. Physica D: Nonlinear Phenomena 133(1):371–389

Mahesh S, Phoenix SL, Beyerlein IJ (2002) Strength distributions and size effects for 2d and 3d composites with weibull fibers in an elastic matrix. International Journal of Fracture 115(1):41–85

Nukala PKV, Simunovic S (2004) An efficient block-circulant preconditioner for simulating fracture using large fuse networks. Journal of Physics A: Mathematical and General 37(6):2093

Nukala PKV, Šimunović S, Guddati MN (2005) An efficient algorithm for modelling progressive damage accumulation in disordered materials. International journal for numerical methods in engineering 62(14):1982–2008

O'Shaughnessy B, Procaccia I (1985) Diffusion on fractals. Physical Review A 32(5):3073

Pfalzner S, Gibbon P (2005) Many-body tree methods in physics. Cambridge University Press

Rezghi M, Eldén L (2011) Diagonalization of tensors with circulant structure. Linear Algebra and its Applications 435(3):422–447

Smith RL (1980) A probability model for fibrous composites with local load sharing. Proceedings of the Royal Society of London A 372(1751):539–553

Zhou S, Curtin W (1995) Failure of fiber composites: a lattice green function model. Acta Metallurgica et Materialia 43(8):3093–3104